San Jose State University

October, 2018

Chromodynamical analysis of lenticular galaxies using globular clusters and planetary nebulae

Emilio J B Zanatta, *Universidade Federal do Rio Grande do Sul*
Arianna Cortesi, *Universidade de Sao Paulo*
Ana L. Chies-Santos, *Universidade Federal do Rio Grande do Sul*
Duncan A. Forbes, *Swinburne University of Technology*
Aaron J. Romanowsky, *San Jose State University*, et al.

Chromodynamical analysis of lenticular galaxies using globular clusters and planetary nebulae

Emilio J. B. Zanatta,[1]⋆ Arianna Cortesi,[2] Ana L. Chies-Santos,[1] Duncan A. Forbes,[3] Aaron J. Romanowsky,[4,5] Adebusola B. Alabi,[5] Lodovico Coccato,[6] Claudia Mendes de Oliveira,[2] Jean P. Brodie[5] and Michael Merrifield[7]

[1]*Departamento de Astronomia, Instituto de Física, Universidade Federal do Rio Grande do Sul, Porto Alegre, R.S., Brazil*
[2]*Departamento de Astronomia, Instituto de Astronomia, Geofísica e Ciencias Atmosfericas da USP, Cidade Universitaria, CEP:05508900, Sao Paulo, SP, Brazil*
[3]*Centre for Astrophysics & Supercomputing, Swinburne University, Hawthorn VIC 3122, Australia*
[4]*Department of Physics and Astronomy, San José State University, San Jose, CA 95192, USA*
[5]*University of California Observatories, 1156 High St., Santa Cruz, CA 95064, USA*
[6]*European Southern Observatory, Karl-Schwarzschild-Strasse 2, D-85748 Garching bei Munchen, Germany*
[7]*School of Physics and Astronomy, University of Nottingham, University Park, Nottingham NG7 2RD, UK*

ABSTRACT

Recovering the origins of lenticular galaxies can shed light on the understanding of galaxy and compare them with the kinematics of planetary nebulae (PNe). The PNe and GC data come from the Planetary Nebulae Spectrograph and the SLUGGS Surveys. Through photometric spheroid-disc decomposition and PNe kinematics. we find the probability for a given GC to belong to either the spheroid or the disc of its host galaxy or be rejected from the model. We find that there is no correlation between the components that the GCs are likely to belong to and their colours. Particularly, for NGC 2768, we find that its red GCs display rotation preferentially at inner radii ($Re < 1$). In the case of the GC system of NGC 3115, we find a group of GCs with similar kinematics that are not likely to belong to either its spheroid or disc. For NGC 7457, we find that 70 per cent of its GCs are likely to belong to the disc. Overall, our results suggest that these galaxies assembled into S0s through different evolutionary paths. Mergers seem to have been very important for NGC 2768 and NGC 3115 while NGC 7457 is more likely to have experienced secular evolution.

Key words: galaxies: structure – galaxies: elliptical and lenticular, cD – galaxies: galaxies: evolution – galaxies: formation – galaxies: kinematics and dynamics – galaxies: star clusters.

1 INTRODUCTION

The morphological evolution of galaxies is an interesting and challenging topic in contemporary astrophysics, where lenticular (S0) galaxies play a central role. The morphology–density relation (Dressler 1980; Dressler et al. 1997; Goto et al. 2003; Postman et al. 2005) and the increase of the number of S0 galaxies at lower redshift, at the expense of the decrease in the number of spiral galaxies in clusters of galaxies (Dressler & Sandage 1983; Whitmore, Gilmore & Jones 1993), led to the idea that S0 galaxies might be the evolutionary products of the transformation of spiral galaxies (Larson, Tinsley & Caldwell 1980). Such evolution would have been driven by environmental effects such as ram pressure stripping, galaxy harassment, mergers, starvation, and like (Gunn & Gott 1972; Abadi,

Moore & Bower 1999; Boselli & Gavazzi 2006). Lenticular galaxies, however, are present in all environments (cluster, groups, and field) (van den Bergh 2009). This widens the evolutionary possibilities for creating a lenticular galaxy and raises questions about their uniqueness as a class: could they be the single final product of a variety of events (Gunn & Gott 1972; Byrd & Valtonen 1990; Quilis, Moore & Bower 2000; Bekki et al. 2005; Bournaud, Jog & Combes 2005; Aragón-Salamanca 2008)?

One proposed scenario is that S0 galaxies may form from spiral galaxies which underwent some form of environment-related process and lost most of their gas and spiral structures. These processes therefore would leave behind a disc structure alongside the spheroidal structure of the bulge and halo (Gunn & Gott 1972; Byrd & Valtonen 1990; Quilis et al. 2000 Bekki et al. 2005; Bournaud et al. 2005; Aragón-Salamanca 2008). Such a scenario would leave the stellar kinematics of the resulting S0 galaxy almost unperturbed,

⋆ E-mail: emiliojbzanatta@ufrgs.br

in comparison with the kinematics of the progenitor spiral galaxy (Aragón-Salamanca, Bedregal & Merrifield 2006; Buta et al. 2010; Cortesi et al. 2013). On the other hand, S0 galaxies have been suggested to also be formed from mergers between galaxies of unequal mass, which would cause an increase in random motions in the stars (Borlaff et al. 2014; Bournaud et al. 2005; Querejeta et al. 2017). Bekki et al. (2005) have shown through simulations that merger events that are able to produce flattened early-type galaxies also are likely to affect the structure and kinematics of the globular cluster (GC) systems associated with such galaxies. Moreover, clumpy disc formation is proposed as a way to form galaxy discs through successive mergers of star-forming clumps (van den Bergh et al. 1996; Elmegreen & Elmegreen 2005; Shapiro, Genzel & Förster Schreiber 2010; Genzel et al. 2011; Ceverino et al. 2015; Garland et al. 2015; Fisher et al. 2017). In fact, simulations such as the ones from Shapiro et al. (2010) and Fisher et al. (2017) show that the formation of GCs in such a condition would happen around $z \approx$ 1-3. Therefore such mechanism could be detected through the kinematics of GCs which would acquire rotation and display disc-like kinematics, even in the halo (Inoue 2013).

About 90 per cent of the total mass and angular momentum of a galaxy resides outside one effective radius (R_e) (Romanowsky & Fall 2012). By exploring the outer regions of galaxies, one may find imprints of their merger histories, and is therefore able to investigate the processes responsible for the build-up of its present mass. However, due to the low surface brightness, galaxy outskirts are expensive to probe. Fortunately, tracers such as globular clusters (GCs) and planetary nebulae (PNe) stand as ideal proxies for the study of the kinematics of such regions (Hui et al. 1995; Coccato et al. 2009; Forbes et al. 2012; Brodie et al. 2014).

GCs and PNe can be detected out to 5-10 R_e in early-type galaxies. PNe present a strong emission in the [OIII] line (5007 Å), which allows one to detect them in regions where the galaxy starlight is very faint. The Planetary Nebulae Spectrograph (PN.S, Douglas et al. (2002)) observed several early-type galaxies, creating catalogues with an average number of over a hundred PNe per galaxy. As shown in Cortesi et al. (2011), this number is enough to recover the stellar kinematics of the galaxy disc and spheroid, since PNe are reliable tracers of the global stellar population of their host galaxy (Coccato et al. 2009; Cortesi et al. 2011). Globular clusters are ubiquitous in early-type galaxies and in the past two decades GC radial velocity catalogues have been acquired for several systems with multi-object spectroscopy in 10m class telescopes (eg. Hanes et al. (2001), Côté et al. (2003), Hwang et al. (2008), Park et al. (2012), Pota et al. (2013) and Forbes et al. (2017)).

The present work analyses the GC systems of three lenticular galaxies in low-density environments (NGC 2768, NGC 3115, and NGC 7457) following the method presented in Cortesi et al. (2016) for the GC system of NGC 1023. Such a study used PNe kinematics derived in Cortesi et al. (2011, 2013).

This paper is structured as follows: in Section 2, we present an overview of the observational data used in this work and the individual galaxies' general properties.

In Section 3, we briefly discuss the method used for probing GC kinematics using GALFIT (Peng et al. 2002), maximum likelihood estimation (MLE), and the kinematics of PNe. In Section 4, we present the results on GC kinematics, in addition to considerations on 1D phase–space diagrams and the radial distribution of GCs and PNe for our sample galaxies. In Section 5, we discuss the results in comparison with the evolutionary paths proposed in the literature for lenticular galaxies. Summary and conclusions are shown in Section 6.

Table 1. Sizes of GC and PN samples used in this work. In the second column, we show the number of the GCs, for each galaxy, for which only photometry is available; in the third column we have the number of GCs for which spectroscopy data are available and in the last column the number of PNe.

Galaxy	N_{GC} Photom.	N_{GC} Spec.	N_{PNe}
NGC 2768	978	106	315
NGC 3115	781	150	188
NGC 7457	536	40	112

2 DATA

In this work, we use spectroscopic and photometric data from GCs and PNe to model the kinematics of a sample of three nearby S0 galaxies. We have selected three non-cluster galaxies so that we could probe their formation mechanisms independently of any process commonly found in high-density environments (e.g. ram pressure stripping). In Table 1, we present the size of the globular cluster and planetary nebula samples, for each galaxy. The spatial distribution of the spectroscopic data is shown on Fig. 1. Additionally, in this section, we describe the sources of the data and briefly discuss the galaxies' basic properties.

2.1 Globular clusters

The GC photometric and spectroscopic data analysed in this work comes from The SAGES Legacy Unifying Globulars and Galaxies (SLUGGS) Survey[1] (Brodie et al. 2014; Forbes et al. 2017). SLUGGS is a wide-field spectroscopic and photometric survey of early-type galaxies undertaken using mainly the Subaru/Suprime-Cam imager and the Keck/DEIMOS spectrograph from the Keck-II-Telescope (Faber et al. 2003). SLUGGS goals revolve around studying the outer regions of early-type galaxies, where stellar light is faint. The survey has deep *gri* imaging and spectroscopy around 8500 Å of 25 nearby early-type galaxies.

The photometric data of all galaxies studied in this work have been described in Pota et al. (2013). The data for NGC 2768 is a combination of Suprime-Cam/Subaru in the $R_C iz$ filters and the Advanced Camera for Surveys (ACS) from the *Hubble Space Telescope* (*HST*).

NGC 3115 data are described in detail in Arnold et al. (2014).The photometric data for this galaxy was obtained with the Subaru/Suprime-Cam in the *gri* FILTERS.[2]

The photometric GC data for NGC 7457 included in SLUGGS comes from Hargis et al. (2011), obtained from observations in the *BVR* filter with the WIYN/MiniMo imager (Saha et al. 2000). Hargis et al. (2011) also obtained spectroscopy for a sample of 20 NGC 7457 GCs, although in this work we use an updated and larger spectroscopic sample for this galaxy's GCs obtained with the Keck/DEIMOS spectrograph and published in Forbes et al. (2017). This new sample has spectroscopy for 40 GCs, which doubles the previously studied spectroscopic sample.

---

[1]http://sluggs.swin.edu.au/Start.html
[2]Additional spectra for NGC 3115 are from the LRIS instrument on the Keck-I-Telescope (Oke et al. 1995) and the IMACS instrument from the Magellan telescope (Dressler et al. 2011).
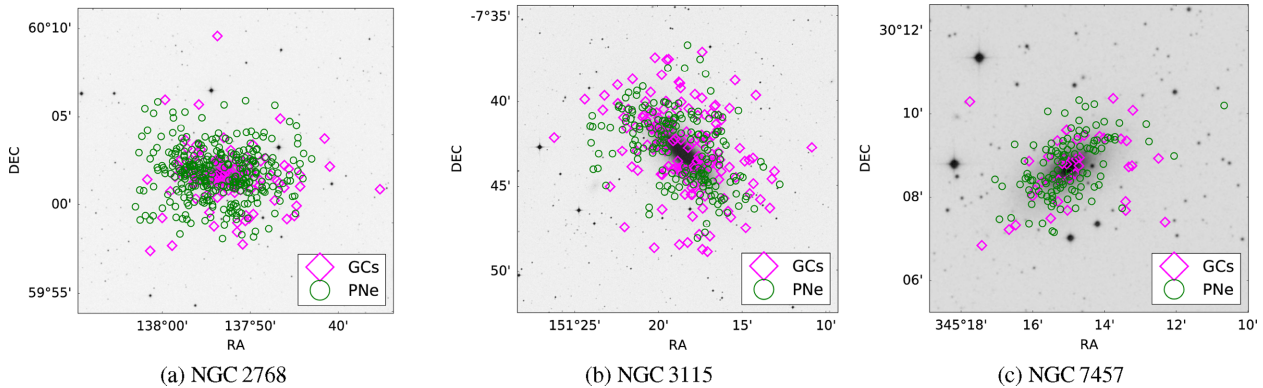
Figure 1. Spectroscopic tracers plotted over K-band images, from 2MASS, of the galaxies in this sample. Magenta diamonds are GCs from Pota et al. (2013) and green circles are PNe from the PN.S catalogue (Douglas et al. 2002).

2.2 Planetary Nebulae

The PNe data for the galaxies studied in this work were obtained with The Planetary Nebulae Spectrograph (PN.S, Douglas et al. (2002)). We also make use of the PNe kinematics obtained in Cortesi et al. (2013) for the galaxies of our sample. The PN.S is a dedicated instrument mounted at the William Herschel Telescope (WHT) in La Palma, Spain. The instrument detects PNe using a technique based on counter-dispersed imaging (CDI), which enables us to obtain velocities and positions for PNe at the same time.

2.3 Galaxies

General properties of the galaxies studied in this work are presented in Table 2. In this section, we further discuss some of their features found in previous works.

2.3.1 NGC 2768

NGC 2768 is a group galaxy classified as an E6 by de Vaucouleurs et al. (1991) and as an S0 1/2 by Sandage & Bedke (1994), located at a distance of about 22 Mpc from us (Tully et al. 2013) in the direction of the constellation of Ursa Major. It is part of the small Lyon group of galaxies 167 (Garcia 1993), and has traces of ionized gas and a dust lane along the minor axis (Kim 1989). It is interesting to add that the ionized gas havs been found to have different kinematics than the stars in the inner regions of the galaxy (Fried & Illingworth 1994). Pota et al. (2013) found a bimodal distribution in colour for the sample of 978 GCs used in this work with a separation at $(Rc - z) = 0.57$ mag, obtained with KMM (Ashman, Bird & Zepf 1994).

The GC system of this galaxy has been previously studied by Pota et al. (2013), who found rotation for the red GCs and negligible rotation for the blue sub-population. Forbes et al. (2012) focused on the red GCs and found that this sub-population follows the radial surface density profile of the galaxy light and is compatible with the kinematics of the bulge component.

2.3.2 NGC 3115

NGC 3115 is the closest S0 galaxy to the MW, with a distance of 9.4 Mpc (Cantiello et al. 2014) and shows the clearer GC colour bimodality of our sample (Brodie et al. 2012; Pota et al. 2013; Arnold et al. 2014; Cantiello et al. 2014). Pota et al. (2013) found a colour separation of photometric GCs at $(g - i) = 0.91$ mag.

This galaxy is located in the field (Brodie et al. 2014) and displays many interesting morphological structures, such as faint remnant spiral structures proposed by Norris et al. (2006) and re-detected recently using VLT/MUSE spectroscopy by Guérou et al. (2016). It has two faint companion galaxies (Doyle et al. 2005).

2.3.3 NGC 7457

NGC 7457 is a field S0 galaxy (Brodie et al. 2014) with a distance of 12.9 Mpc (Alabi et al. 2017). In contrast with the other galaxies in this sample, it shows no signs of bimodality in its GC population (Hargis et al. 2011; Pota et al. 2013). Previous studies of this galaxy also proposed a counter-rotating galaxy core (Sil'chenko et al. 2002) and a possible major merger origin (Hargis et al. 2011). Furthermore, it presents the smallest amount of GCs of all galaxies in the sample, with a total number of $\sim 210 \pm 30$ GCs (Hargis et al. 2011).

3 METHODS AND ANALYSIS

In most galaxies, GCs can be separated into two sub-populations based on optical colour and metallicity, namely a red metal-rich population and a blue and metal-poor one. Different scenarios were proposed to explain the evolution of such sub-populations within an evolving galaxy, such as blue GCs being commonly found in the halo (Forbes, Brodie & Grillmair 1997), while red GCs are likely associated with the bulge, since they formed in a later phase along with the spheroidal component or migrated towards the centre of the galaxy after the gas-rich phase of galaxy evolution (Shapiro et al. 2010). By studying the GC kinematics we can find signatures of their origins, if they show a disc or spheroid-like behaviour. To reach this goal, we need to recover the probability for every GC to belong to the galaxy as modelled with PNe, and to a given galaxy component. In this section, we will describe all the steps needed to retrieve these probabilities.

3.1 Spheroid-disc decomposition and photometricprobabilities

Cortesi et al. (2013) performed a photometric decomposition of the light of the galaxies in our sample, using a model comprising a disc and a spheroidal component (i.e. bulge and halo) and K-band images from the 2MASS catalogue (Skrutskie et al. 2006). Using these results, we compare the light profiles of these galaxies with the radial number density of their associated GCs, as shown in Fig. 2.

Table 2. General properties of the galaxies published in Alabi et al. (2017). From left to right, the columns are: Galaxy designation, distance, systemic velocity, central stellar velocity dispersion within 1 kpc, ellipticity, environment (F=Field, G=Group), galaxy morphology from Brodie et al. (2014), average luminosity-weighted age of the stellar population within 1 R_e from McDermid et al. (2015), effective radius, stellar mass, and bulge-to-total light ratio from Cortesi et al. (2013).

Galaxy	Dist. (Mpc)	V_{sys} (km/s)	σ_{1kpc} (km/s)	ϵ	env.	morph.	Age (Gyr)	R_e (kpc)	$\log(M_*)$ (M⊙)	B/T
NGC 1023 †	11.1	602	183	0.63	F	S0	12.3	2.58	10.99	0.53
NGC 2768	21.8	1353	206	0.57	G	E/S0	12.3	6.37	11.21	0.71
NGC 3115	9.4	663	248	0.66	F	S0	9.0	1.66	10.93	0.74
NGC 7457	12.9	844	74	0.47	F	S0	3.8	2.13	10.13	0.30

Note: † GCs and PNe kinematic analysis for this galaxy was done in Cortesi et al. (2016) with the same method used in this work.

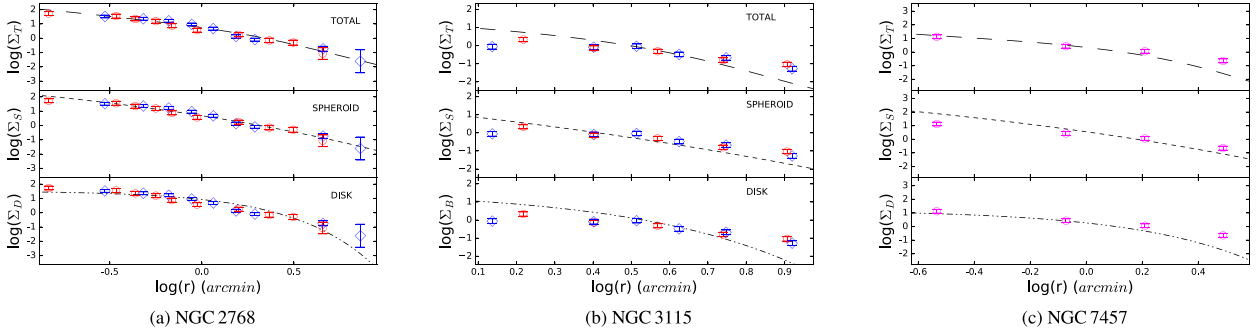(a) NGC 2768   (b) NGC 3115   (c) NGC 7457

Figure 2. Photometric GC number density profiles (open diamonds) and galaxies' surface brightness profiles (following the GALFIT fit from Cortesi et al. (2013)). Top panels compare photometric GC number density profiles with the total light profiles, while centre and lower panels compare the GC number density with spheroid and disc light profiles, respectively. For NGC 2768 and NGC 3115, both blue and red GC populations are shown, represented by red circles and blue diamonds, respectively, while for NGC 7457 only the total population of GCs is shown, represented by magenta open diamonds. The light profile curves have been arbitrarily shifted along the y-axis to better match the GC number density in each panel. There is a slightly better comparison between GCs and spheroid profiles for all galaxies, although disc profiles also show a good agreement with GC density except at large radii. There is no clear difference between red and blue GCs.

For NGC 2768 and NGC 7457, GC radial number densities follow reasonably well, within errors, the light profiles of the galaxies and of their components. In the case of NGC 3115, there is, however, a less obvious compatibility between GC density and the spheroid radial light profile. While the inner discrepancy might be due to incompleteness, i.e. the GCs get lost against the galaxy light in the central regions, at large radii, such difference might arise from treating the halo and the bulge as a single component in the model.

In general, a disc and a spheroidal component are a good approximation to model the light of S0 galaxies. It is to be noted, nevertheless, that some galaxies have slightly more complex structures, and that the images used for the decomposition might be too faint to account for the halo component of the galaxy. Therefore, such a decomposition is prone to several systematic uncertainties and multiple approaches, such as the ones in Savorgnan & Graham (2016) for NGC 1023 and NGC 3115. For the purpose of studying the kinematics of GC systems and PNe, the decomposition performed in Cortesi et al. (2013) is reasonable enough.

With the spheroid-disc light decomposition recovered in Cortesi et al. (2013), we also obtain preliminary photometric probabilities, f_i, for each tracer to belong to the spheroid model. We create an image dividing the spheroid by the total model of the galaxy light and we calculate the flux at the location of every GC in such image, within a circular aperture of radius equal to 3 pixels. To obtain the final probabilities of a GC to belong to the spheroid or the disc we combine f_i with the the GCs' kinematics, which will account for possible degeneracy or lack of precision of the photometric model (Cortesi et al. 2011) (see Section 3.3).

3.2 Kinematics

In Fig. 3, we show the smoothed velocity maps for the GC systems, obtained using Adaptive Kernel Smoothing (see Coccato et al. (2009) for details on using the technique). We detect clear rotation as measured from the GC systems for all galaxies. For NGC 3115, this is true for both red and blue sub-populations, while we can notice that for the case of NGC 2768 the rotation is supported by the inner red GCs.

To recover the kinematics of the GC and PNe systems of the galaxies in this work, we use Maximum Likelihood Estimation to find the best-fitting kinematic parameters, θ, assuming a Gaussian velocity distribution for its GCs or PNe populations:

$$F(v_i; \theta) \propto \exp\left[-\frac{(v_i - V_{los}(V))^2}{2\sigma^2}\right] \quad (1)$$

where v_i are the velocities of the discrete tracers, V_{los} is the galaxy line-of-sight velocity, V is the fitted rotation velocity, and σ is the fitted dispersion velocity. We bin the data in elliptical annuli with the same ellipticity of the disc component for each galaxy (see Table 2), and with approximately the same number of objects in every bin. In this way, we recover the kinematic profile with radius. Moreover, we iterate the MLE fit until all objects are within the 2.3 σ confidence interval, discarding outliers in each run. This ensures the robustness of the fit even when dealing with a possible significant number of outliers (for example, accreted GCs).

In Fig. 4, we present the results of the likelihood analysis for GCs and PNe. As far as the rotational velocity is concerned, the galaxies have very distinct profiles: NGC 2768 has strong kinematic dis-
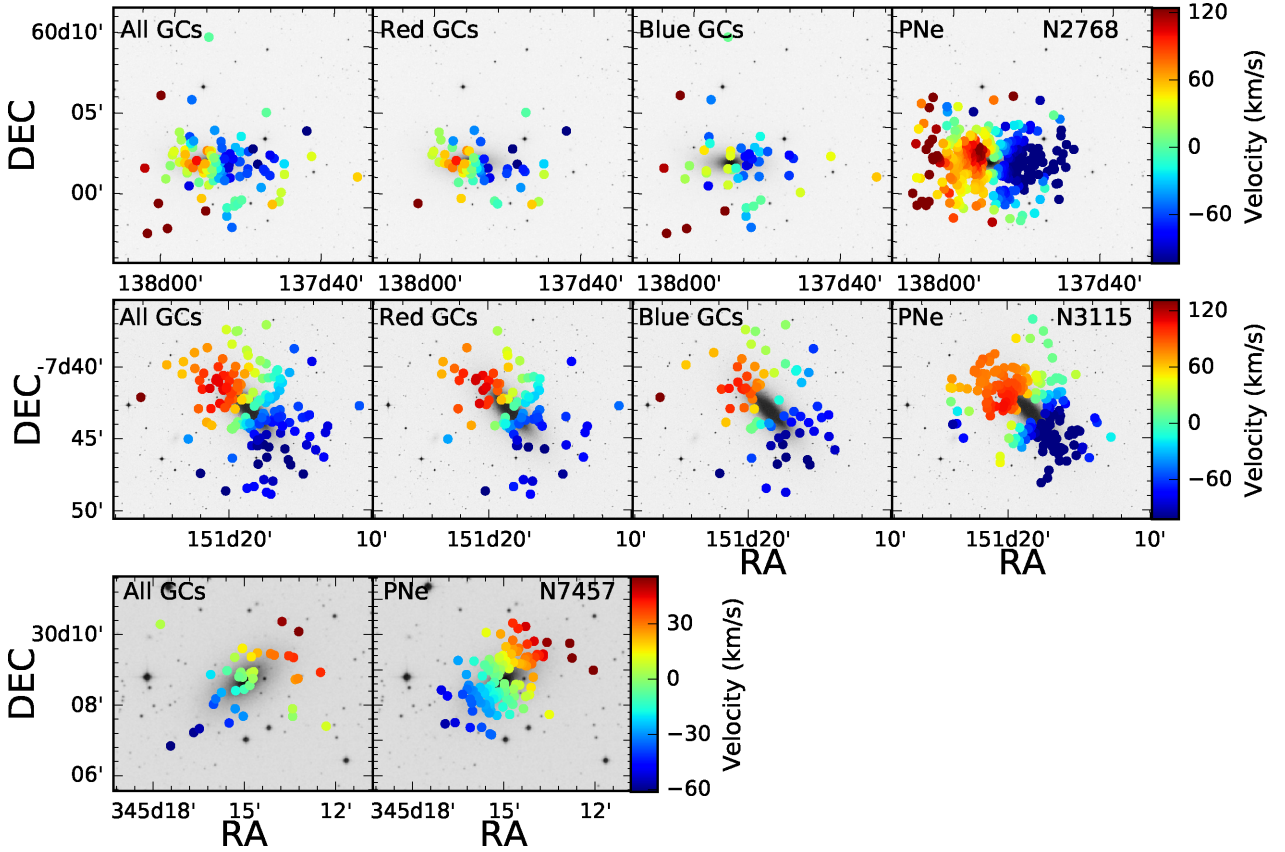
Figure 3. Smoothed velocity maps of sample galaxies PNe and GC populations, using Adaptive Kernel Smoothing (Coccato et al. 2009). For all galaxies, rotation can be detected. However, most of the apparent rotation of the GC system of NGC 2768 seems to be concentrated towards the centre and to be due to its red sub-population. NGC 7457 has no signs of clear GC colour bimodality so the whole GC sample is shown.

crepancies between its GC colour sub-populations, with red GCs showing rotation around 100 km s⁻¹ and blue GCs showing negligible rotation. The rotational velocity of the GCs in NGC 3115 decreases with radius consistently and independently of colour, as found for NGC 1023 in Cortesi et al. (2016). For this galaxy, we also note that the rotational velocities of the PNe and GCs are consistent, despite the aforementioned model limitations. Lastly, the GCs of NGC 7457 show a flatter rotational profile for both GCs and PNe. For the velocity dispersion, all galaxies show good agreement between PNe and GCs. This is expected since they share the same gravitational potential.

3.3 Final probabilities using photometry and PNe kinematics

In this section, we summarize the method introduced by Cortesi et al. (2016), and refer the reader to such work for further details.

In Cortesi et al. (2013), the kinematics of the bulge and the disc of the galaxies in this work were modelled using a MLE fitting of the PNe velocity field. Using such kinematic models, we can derive the probabilities that every GC belongs to the galaxy disc or spheroid, solving the following equation:

$$
\mathcal{L}(v_i; V, \sigma_r, \sigma_\phi, \sigma_{\mathrm{sph}}) \propto \frac{f_i}{\sigma_{\mathrm{sph}}} \exp\left[-\frac{v_i^2}{2\sigma_{\mathrm{sph}}^2}\right]
$$

$$
+ \frac{1 - f_i}{\sigma_{\mathrm{los}}(\sigma_r, \sigma_\phi)} \exp\left[-\frac{(v_i - V_{\mathrm{los}}(V))^2}{2\sigma_{\mathrm{los}}(\sigma_r, \sigma_\phi)^2}\right]. \quad (2)
$$

where v_i are the individual GC velocities, V is the galaxy rotational velocity as derived from PNe, V_{los} and σ_{los} are the line-of-sight velocity and dispersion velocity, respectively. The radial and azimuthal components of the velocity dispersion of the disc component are given by σ_r and σ_ϕ, while σ_{sph} is the dispersion velocity for the spheroid component (also derived from PNe). The f_i values are the probabilities obtained in Section 3.1 for every GC to belong to the galaxy spheroid component based on photometry only.

In Fig. 5, we show the recovered probabilities of the GCs to belong to the spheroid, $\mathcal{L}_{sph}(v_i, f_i)$, obtained normalizing the first term on the right-side of equation (2), in comparison with the probabilities to belong to the spheroid retrieved from the photometry only, f_i. We notice a decrease in probability values around 0.5 present in the histogram that show probabilities obtained from photometry only, in comparison with the probabilities obtained with photometry and kinematics. This shows the core improvement of the MLE method over the photometric probability approach justifying our choice of a simple bulge-disc decomposition.

We calculate the total number of GCs that belong to the galaxy disc or spheroid by summing-up the probabilities $L_{sph}(v_i, f_i)$ and the total number of disc GCs is obtained summing $(1-L_{sph}(v_i, f_i))$. These values are outlined in Table 3, for the total, red and blue sub-populations.
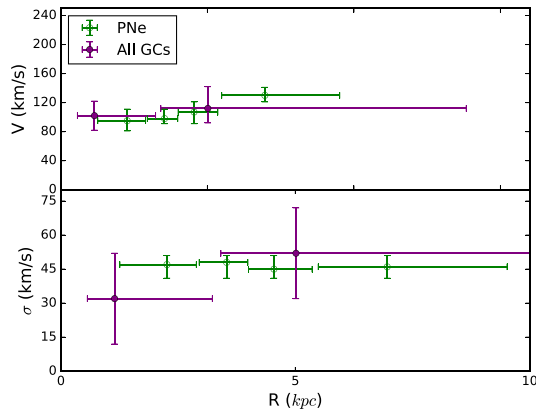
Moreover, the likelihood fit also offers us the advantage of detecting objects that are outliers, i.e. not likely to be compatible with the host galaxy kinematics, as traced by PNe in Cortesi et al. (2013).
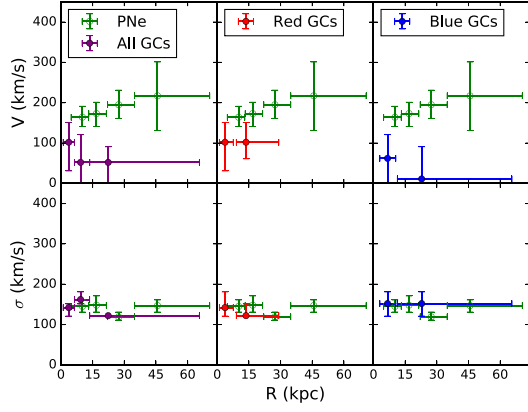
(a) NGC 2768
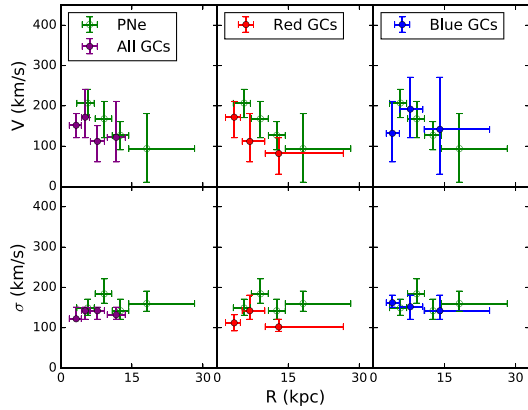
(b) NGC 3115

(c) NGC 7457

Figure 4. Rotation profiles and velocity dispersion for GCs and PNe obtained through the likelihood analysis, considering a one-component kinematic model. Vertical error bars are uncertainties and horizontal error bars represent bin-sizes. The data were divided in elliptical bins along circularized radius with approximately the same number of objects in each bin. The number of bins for each GC sub-population was designed aiming to ensure enough objects in each bin for the likelihood estimation. Note the distinct behaviour between the blue and red GC colour sub-populations of NGC 2768 and the diverse trends for the kinematics of the different GC systems.

We set the likelihood threshold at 2.3σ (see Cortesi et al. (2016)). Within the entire GC spectroscopic sample, such objects account for 10 GCs in NGC 2768, 32 GCs in NGC 3115 and 4 GCs in NGC 7457. This means that 21.5 per cent of NGC 3115 GCs are not likely to be compatible with the galaxy model (previously obtained with PNe and the K-band image). Therefore we can explain such objects in two ways. One possibility is that they might have been recently accreted. Another option is that they might just belong to the galaxy halo, which is not separately included in this study, but is treated together with the bulge as a single spheroidal component. Nevertheless, this number of rejected objects in NGC 3115 is a higher amount than the 9.4 per cent rejected objects in NGC 2768 and 10 per cent in NGC 7457.

4 RESULTS

4.1 Colour and kinematics

In Fig. 6, we show the radial distribution of GCs versus their colours, colour-coded according to their probability of belonging to the spheroid, $L_{Sph}(v_i, f_i)$.

Fig. 6 clearly shows that we are looking at three galaxies with very distinct GC systems. As mentioned in Section 2, NGC 3115 is clearly bimodal in colour, similarly to NGC 2768, while NGC 7457 shows no bimodality in colour for its GCs. Moreover, for NGC 2768 17 per cent of GCs are associated with the disc component while NGC 3115 has a similar number of disc-like and spheroid-like GCs, and NGC 7457 has 15 per cent GCs associated with the spheroid component. We find no correlation between the colours of the GCs and their kinematics, since in NGC 2768 both the populations of red and blue GCs have spheroid-like kinematics[3]. In NGC 3115 there are blue and red GCs associated with both the spheroid and the disc. For NGC 7457, the GC system does not appear bimodal neither in colour nor kinematics. For comparison, NGC 1023 have 19 red and 18.6 blue GCs belonging to the disc, along 13 red and 25.4 blue GCs belonging to the spheroid (Cortesi et al. 2016). On the other hand, we notice that most of the GCs that are more likely to have disc-like kinematics are located in the inner regions of the galaxies, within 10 kpc. It is possible, however, to find some disc-like GCs at larger radii ($r > 5R_e$). For all galaxies, rejected GCs are scattered in the plot, suggesting no correlation among colour, kinematics, and radius. Those objects will be discussed in more detail in the following section.

4.2 1D phase–space diagrams

It is interesting to combine 1D phase–space diagrams of the GCs with the information obtained from their recovered probabilities of being associated with the disc or the spheroid. In Fig. 7, we use the quantity $\Delta V = V_{los} - V_{sys}$, where V_{sys} is the systemic velocity of a given galaxy, as listed in Table 2, versus galactocentric radius and in Fig. 8 Δx, the projected distance along the galaxy's major axis. We overplot the PNe for comparison.

In the 1D phase–space diagrams, GCs that are bound to the system create a 'bell shaped' pattern (see Rocha, Peter & Bullock (2012)). Spheroid-like objects would lie approximately along the line where $\Delta V = 0$, since they have no net rotation, just a natural scatter due to their hot kinematics. On the other hand, disc objects, due

---

[3]See discussion in Section3.3 and Fig. 4 about differences between the red and blue GCs kinematics regarding the rotation profiles
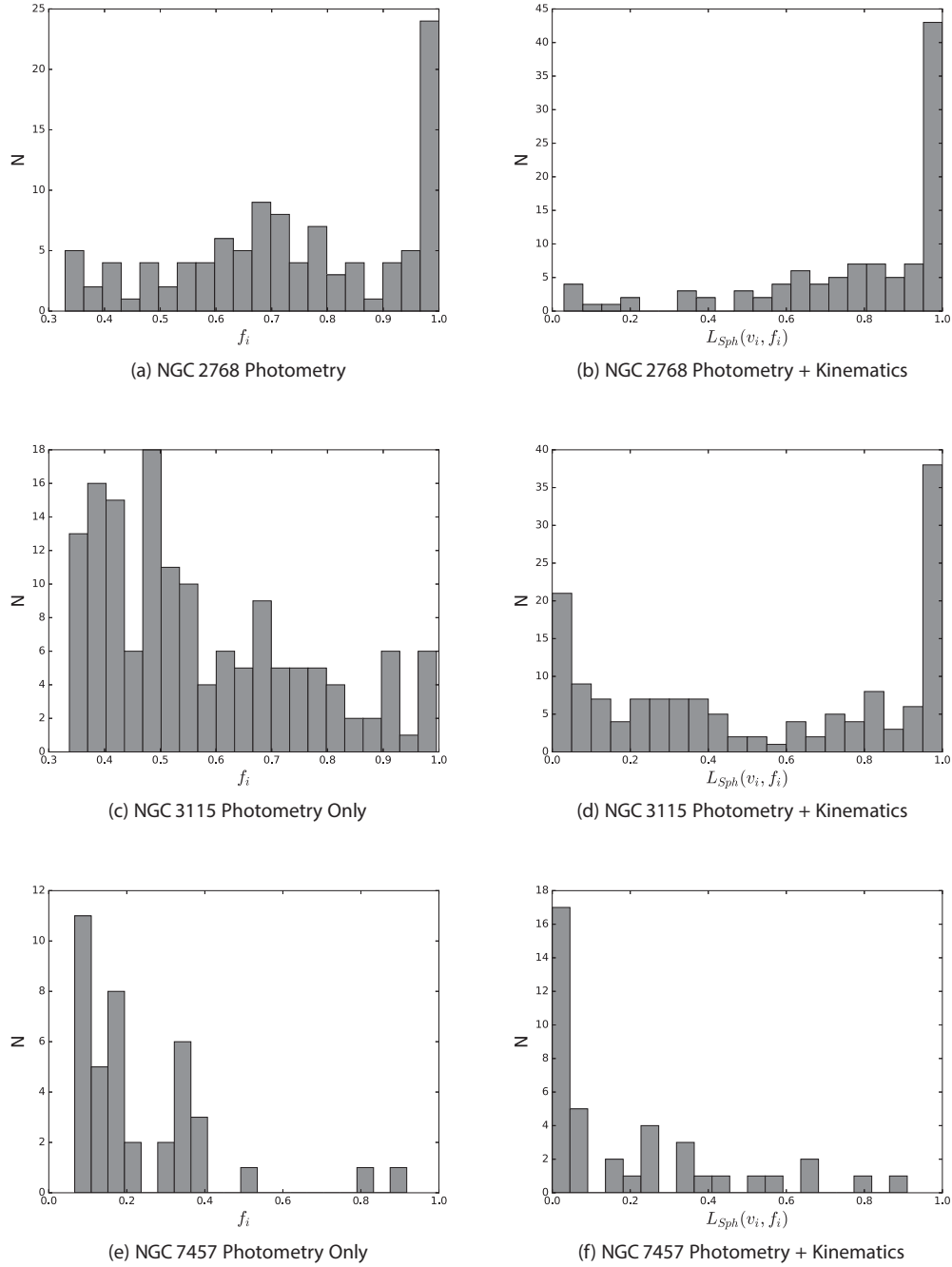
Figure 5. The probability of GCs belonging to the host galaxy spheroid. *Left-hand panels* : probabilities from photometry, f_i; *right panels* : probabilities from photometry and kinematics, $L_{sph}(v_i, f_i)$. Notice the decrease of objects with probability values around 0.5 in the right panels compared to the left ones, showcasing the improvement of adding kinematic information to the photometric analysis. Also, notice the diverse cases presented in the right-side panels. Most of NGC 2768 GCs are likely to belong to the spheroid, while NGC 3115 has a significant number of GCs likely to be in the disc, as well as in the spheroid, and finally NGC 7457 shows a dominant disc-like population of GCs.

Table 3. Number of GCs associated with each of the host galaxy components, following the kinematic analysis described in Section 3.2. GCs are also divided by colour sub-populations in the case of NGC 2768 and NGC 3115.

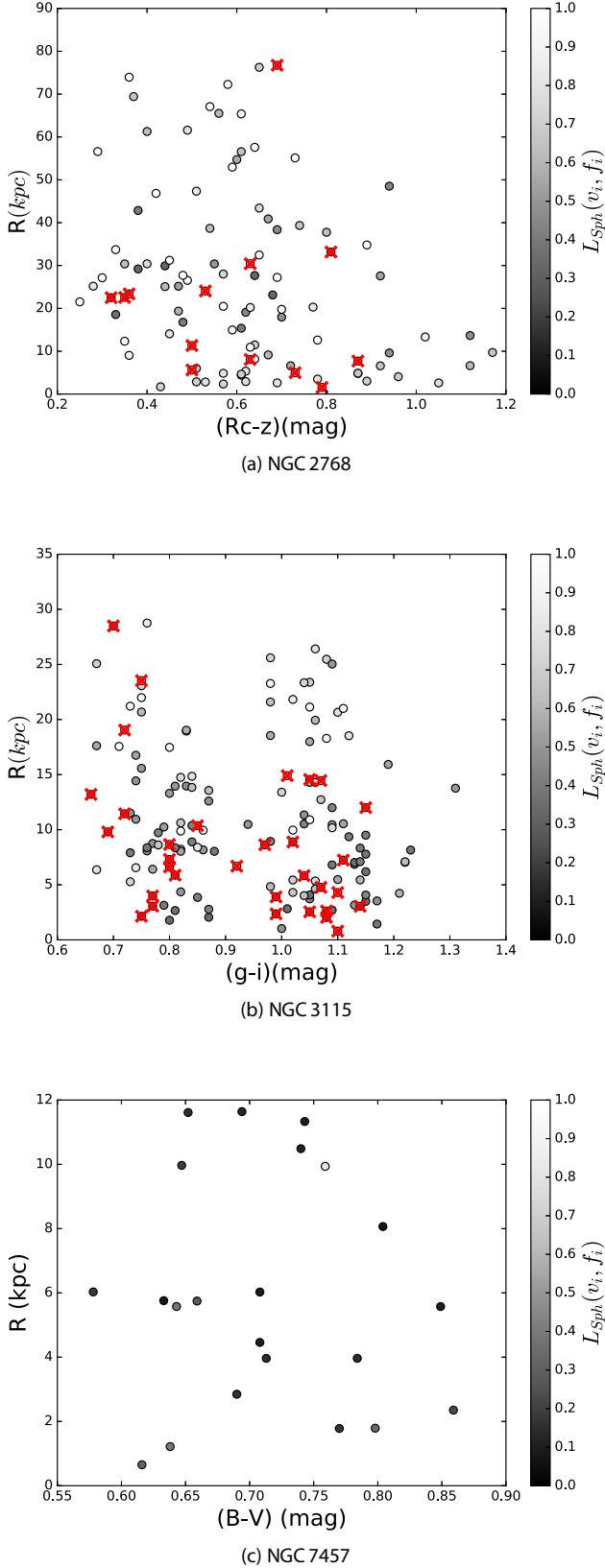| Galaxies	Disc			Spheroid		
	Red GCs	Blue GCs	Total	Red GCs	Blue GCs	Total
NGC 2768	14.8	10.0	24.8	40.2	27.9	68.1
NGC 3115	26.8	21.4	48.2	37.2	31.5	68.7
NGC 7457	-	-	27.3	-	-	8.8

Figure 6. Radial distribution of GCs, colour coded by $L_{Sph}(v_i,f_i)$, the probability of belonging to the spheroid. Red X-shaped markers represent rejected objects with kinematics not compatible with their host galaxy kinematics following the likelihood analysis. For NGC 7457 we lack colour information for some GCs. Therefore the rejected objects are not shown.
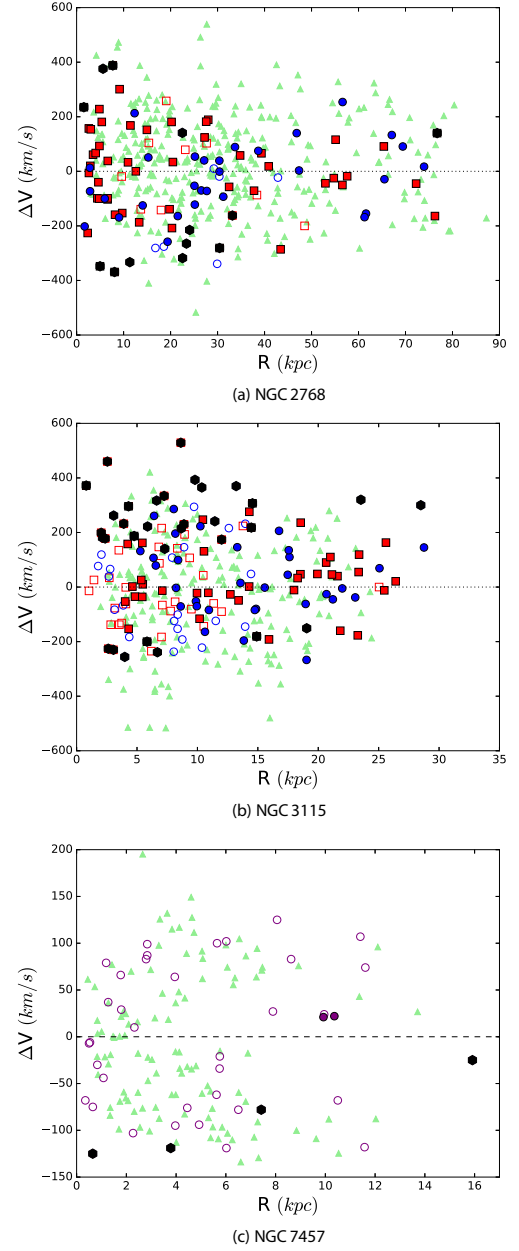

Figure 7. 1D phase–space diagrams for GCs and PNe. Blue and red GCs are represented by blue circles and red squares, respectively. GCs likely to belong to the spheroid are represented by filled markers, and GCs with high probability of being part of the disc are represented by open markers. Green filled triangles are PNe. For NGC 7457, due to its lack of bimodality in colour, we show only disc and spheroid populations. Objects marked as black hexagons are rejections from the kinematic fit.

to their larger rotational velocities, would show up symmetrically around the galaxy's systemic velocity. Moreover, the broader the distribution around the systemic velocity of the galaxy, the higher the random motions. For instance, objects recently accreted onto the system would generally lie at the outer part of the distribution given that they may not have reached equilibrium yet, with respect to its new host galaxy kinematics (see also Rhee et al. (2017)).

Fig. 7 shows the 1D phase–space diagrams for NGC 2768, NGC 3115 and NGC 7457. We divide the GCs between disc and spheroid using a value of $L_{Sph}(v_i,f_i) = 0.5$. Note that there is a
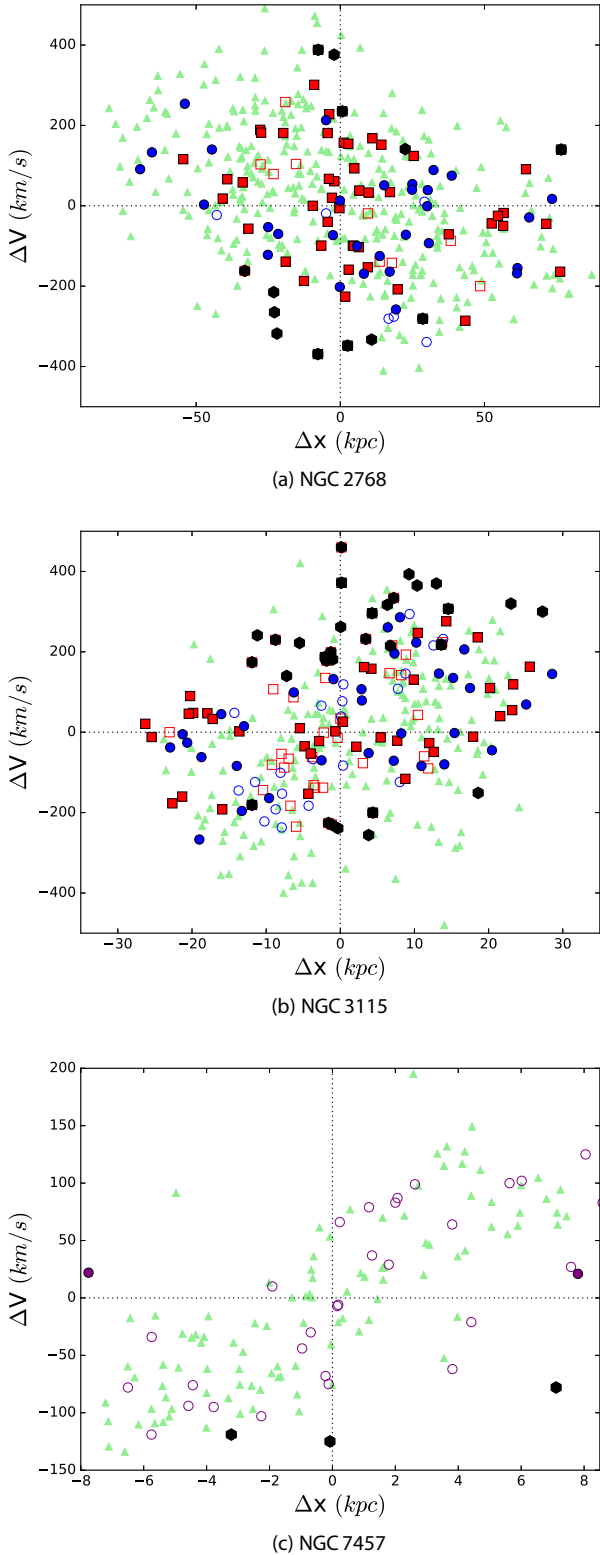
(a) NGC 2768

(b) NGC 3115

(c) NGC 7457

Figure 8. Velocity versus distance along the major axis for GCs and PNe. Markers are the same as in Fig. 7 for all panels. Notice the grouping of rejected GCs in NGC 3115 around δ V $\approx 300\,\mathrm{km\,s^{-1}}$.

concentration of red GCs towards the centre of NGC 2768, within $1R_e$ (6.37 Kpc) Fig. 7 (a). However, as seen in Fig. 6 (a), both red and blue sub-populations show high probabilities of belonging to the spheroid. Forbes et al. (2012) when studying this galaxy kinematics, specifically looking into its red GC population, found that it is related to the kinematics of the galaxy's spheroid. Therefore, it is reasonable to say that, as blue GCs in this galaxy have a high probability of being in the spheroid and are generally not present at the same radii as the red GCs, they are likely located predominantly in the halo.

In the 1D phase–space diagram for GCs and PNe of NGC 3115, Fig. 7 (b), one can see a transition from disc-like GCs to spheroid-like GCs with radius. Rejected objects (black markers) from the likelihood analysis also display an interesting distribution in the diagram. Most of them have similar values of ΔV, around $200\,\mathrm{km\,s^{-1}}$.

These GCs might form a group that could have an *ex-situ* origin.

For NGC 7457, by analysing Fig. 7 (c), we see a more compact distribution of GCs and PNe in the phase–space diagram if compared to panels (a) and (b), with objects showing values of $\Delta V \leq 200\,\mathrm{km\,s^{-1}}$. NGC 2768 and NGC 3115 have GCs with values of ΔV in the range of $600\,\mathrm{km\,s^{-1}}$, therefore, NGC 7457 shows lower velocity dispersion, as expected given the recovered kinematics (see Fig. 4). GCs and PNe have a high probability of belonging to the disc of the galaxy and share the same loci in this plot. They show a U' shaped distribution. This shape might be due to the very low number of GCs and PNe with hot kinematics, consistent with the galaxy being disc dominated (Cortesi et al. 2013). This galaxy seems to generally lack a hot kinematic component in its outer regions, beyond around $2\,R_e$, quite differently from NGC 2768 and NGC 3115 which have, in fact, more prominent bulges and are more massive than NGC 7457.

In addition to Fig. 7, it is interesting to analyse the distribution of the velocities of the tracers versus the projected distance along the major axis of the host galaxies, see Fig. 8. The rejected GCs of NGC 3115 show interesting properties. In fact, they seem to form a coherent structure, reinforcing what was found in Fig. 7.

Finally, NGC 7457 shows a strong disc-like shaped distribution in Fig. 8, both for PNe and GCs. This was already expected given the rotation profiles in Fig. 4, where PNe and GCs show similar kinematics.

5 DISCUSSION

In this section, we analyse the GC rotation profiles and the V/σ ratio of the GCs and we compare our results with simulations. The V/σ quantity can be used as an indicator of how much the kinematics of a galaxy's GC system is dominated by rotational velocity, in the case of values higher than 1, or is more influenced by random motions, in the case of a ratio smaller than 1.

Bekki et al. (2005) studied with dissipationless numerical simulations the outcome of various merger scenarios on the GC kinematics of early-type galaxies. They showed that mergers with a proportion of 10:1 are able to produce flattened early-type galaxies, such as lenticulars, and they would impact the kinematics of GCs in such a way that their rotation at large radii would be weaker than at small radii. Bournaud et al. (2005) showed that minor mergers with a proportion of 4.5:1 would produce a stellar disc with $V/\sigma \approx 1$ for the remnant galaxy and a merger with a proportion of 10:1, such as the ones Bekki et al. (2005) studied, would produce a stellar disc
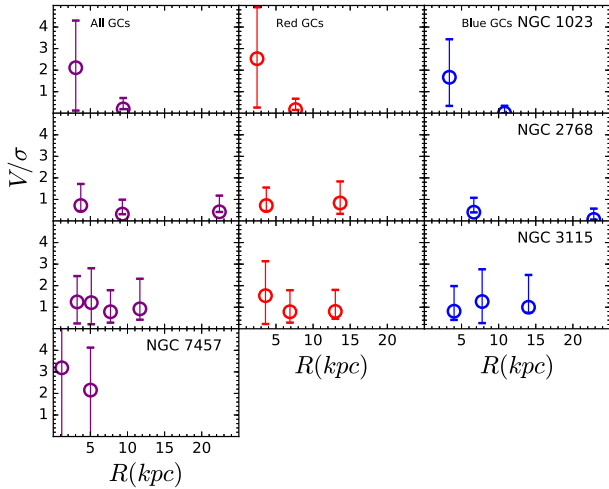
Figure 9. V/σ ratio obtained from GCs, with the addition of NGC 1023 from Cortesi et al. (2016). *Left*, full sample of GCs for each galaxy, *centre* : red subpopulation of GCs, *right* : blue subpopulation of GCs. NGC 7457 has no signs of significant bimodality so only one population is shown. The error bars for NGC 7457 GCs are in the order of $\delta V/\sigma \approx \pm 3.0$, due to the uncertainties in recovering σ. Note that these values are obtained assuming only one component and not separating disc-like from spheroid-like objects.

with $V/\sigma \approx 2$. Besides a major merger event[4], another likely path on the evolution of galaxies is a sequence of minor mergers. On the other hand, Moody et al. (2014) showed that multiple minor mergers would not produce fast rotating galaxies (Emsellem et al. 2011), but instead would be more likely to produce hot, elliptical and slow rotating galaxies.

In Fig. 9, we show the V/σ ratios obtained from the GC subpopulations using the method described in Section 3 and the results from Fig. 4. One can see that the values of V/σ for NGC 3115 are close to or smaller than 1 for both GC sub-populations and for all radii, which would support the scenario in which this galaxy is a remnant of a merger event where the masses involved follow at least a 4.5:1 proportion. This merger would not have been strong enough to rip the disc structure of the galaxy apart, but would be significant enough to accelerate the gas removal or consumption within the galaxy.

The signs of remnant spiral star forming structures hypothesized by (Norris, Sharples & Kuntschner 2006; Guérou et al. 2016) support this formation scenario, where the progenitor of NGC 3115 was a spiral galaxy that later merged with a smaller companion. In Cortesi et al. (2016), it was argued that for NGC 1023 the ratio between the rotation velocity and the velocity dispersion in the azimuthal direction is not compatible with a faded spiral galaxy. It was, instead, suggested that NGC 1023 formed at redshift $\simeq 2$, through the merger of clumps (Inoue 2013). If one compares Fig. 6 of Cortesi et al. (2016) with Fig. 4 of this work, it is notable for the similarity between the red GCs of NGC 3115 and NGC 1023. Hence, clumpy disc formation can also be a scenario to explain the kinematics of the red GC population and the higher fraction of GCs with disclike kinematics in NGC 3115. Nevertheless, NGC 3115 has a higher B/T ratio when compared to NGC 1023 (Cortesi et al. 2016). Thus, this galaxy is more consistent with having gone through a series of minor mergers (see also Arnold et al. (2014)).

[4]Bekki et al. (2005) considers mergers with galaxies of masses in the proportion of 4.5:1 as major mergers.

The results for NGC 2768 point to a very different scenario compared to the other three galaxies.

Forbes et al. (2012) argued that the radial distribution of the V/σ ratio of red GCs in this galaxy is similar to the one of spheroid PNe and stars, as found in spiral galaxies. Furthermore, we find that for the GCs the V/σ ratio is ≤ 1 at all radii, independently of the sub-population considered. According to Bekki et al. (2005), such values of V/σ are the result of a 4.5:1 merger, which is consistent with the galaxy having a more prominent spheroidal structure and a high amount of GCs associated with its spheroid.

Although we are not able to set a single hypothesis for the origin and evolution of NGC 2768, it is clear from our results that its origin differs from that of NGC 3115 and NGC 1023.

NGC 7457 is a peculiar galaxy, since, unlike the others in the sample, ~ 70 per cent of the GCs are located in the disc. This galaxy has the fewest number of GCs overall (around 210, see Hargis et al. (2011)). Moreover, we only have spectroscopy for 40 of those, and therefore a slightly less reliable likelihood fit. Nevertheless, the results from the rotation profiles based on GCs are in good agreement with the results for PNe published in Cortesi et al. (2013), who analysed a sample of 113 such objects. In addition, Hargis et al. (2011) studied the GC system of NGC 7457 and concluded that although the spatial distribution of the system is very elliptical, an inclined disc GC population could explain the observations. In the same work, it was suggested that the most likely formation scenario for this galaxy is through a merger event involving galaxies with unequal masses. NGC 7457 is a field galaxy, so gas stripping mechanisms, which are usually related to dense environments, are very unlikely to be major contributors here. Even so, it could be the result of starvation, where the isolated galaxy, after consuming all its gas reservoir, slowly stops creating young stars (Bekki, Couch & Shioya 2002). Presently, in the literature, scenarios for earlytype galaxy formation involving a two-phase evolution are gaining popularity (Oser et al. 2010). In these scenarios, the bimodality of GCs in colour, metallicity and age would be a more natural outcome. Hargis et al. (2011) and Pota et al. (2013) were not able to detect bimodality in colour for the GCs in this galaxy (but see Peacock et al. 2017).

The V/σ ratio for this galaxy is more than 2, which would mean, following Bournaud et al. (2005), that, at most, it has undergone a merger event with a proportion of around 10:1. Moreover, the simulations of Bekki et al. (2005) indicate that the GC systems of galaxies that suffered minor mergers, as the one that would form flattened disc galaxies, such as NGC 7457, should retain a more spherical structure with little rotation at larger radii, which does not seem to be the case here. Another piece of information that can be added to this puzzle comes from Alabi et al. (2017). In this work, the dark matter fraction at large radii for NGC 7457 was found to be around 0.9, within $5 R_e$. This is greater than the dark matter fraction values found for NGC 2768, NGC 3115, and NGC 1023 which are all around 0.6. With this information, Alabi et al. (2017) calculated an assembly epoch for the halo of NGC 7457 at $z \approx 4.4 \pm 1.1$, or 12.3 Gyr ago. However, the mean luminosity-weighted ages for the stellar content of the central regions of this galaxy and of some of its GCs are around 3-7 Gyr (Sil'chenko et al. 2002; Chomiuk, Strader & Brodie 2008; McDermid et al. 2015). Therefore, the assembly of the halo of the galaxy would have taken place long before some of the GCs and stars at the centre of the galaxy were created. This formation scenario is compatible with a secular evolution scenario, with no mergers at least after $z \simeq 4$. However, clumpy disc formation can also explain the fact that NGC 7457 has a disc-dominated GC population (Inoue 2013).
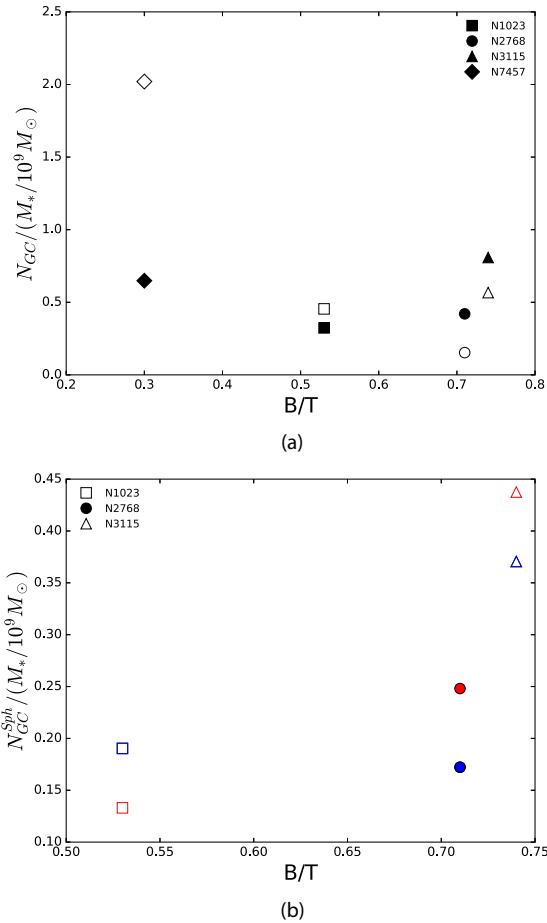
Figure 10. *Upper panel:* Comparison between the number of GCs in the spheroid (filled markers) and the disc (open markers) of our sample galaxies, divided by total stellar mass (M_*) and the bulge-to-total ratio of the galaxy light profile, as obtained in Cortesi et al. (2013). *Lower panel:* Same as the upper panel, but only accounting for the spheroidal GC population of all galaxies, with the exception of NGC 7457, and separated in red and blue colour subpopulations.

In Fig. 10 (a), we compare the number of GCs associated with the spheroid or disc components of its host galaxy, normalized by total stellar mass, with the bulge-to-total (B/T) ratio of the host galaxy light profile from Cortesi et al. (2013). We do not find that the number of GCs increases with the host galaxy B/T ratio. Nevertheless, if we consider only the number of GCs that belong to the spheroid (in panel b[5]), we can see a trend with B/T. This suggests that the number of spheroidal GCs in a given galaxy can be estimated by its photometric properties, such as the fraction of bulge light, but disc GCs, on the other hand, do not follow a similar relation. This discrepancy with disc GCs then impacts the total number of GCs of a given galaxy when compared to its B/T ratio and should not be ignored. On a final note, Fig. 10 (a) also showcases the unusual proportion of GCs in NGC 7457 in proportion to its mass when compared to the other galaxies.

---

[5]NGC 7457 is left out due to is negligible amount of spheroidal GCs, when compared to the other three galaxies.

6 SUMMARY AND CONCLUSIONS

In this work, we recovered the kinematics of the GC systems of three lenticular galaxies in low density environments: NGC 2768, NGC 3115, and NGC 7457. We employed the method presented in Cortesi et al. (2016) for NGC 1023 to obtain the probability of every GC to belong to the disc or the spheroid of the galaxy, using PNe kinematics and K-band photometry. The results point to a different formation scenario for each galaxy. NGC 2768 hosts a very prominent spheroidal GC population. NGC 3115 has the same number of GCs associated with the disc and the spheroid components. NGC 7457, interestingly, at least for the sample used in this work, has the majority of its GCs compatible with disc-like kinematics.

Following the simulations of Bekki et al. (2005) and Bournaud et al. (2005), and the fact that all galaxies in this sample are isolated or in small groups, we investigated the possibilities of merger origins for the galaxies studied. Although such hypothesis remains reasonable, the kinematics of red GCs associated with the disc component are compatible with clumpy disc formation. In the case of NGC 7457, our results seem to point towards a secular evolution from a regular spiral galaxy, or clumpy disc formation. Also of interest, the GC colour sub-populations of NGC 2768 display distinct kinematic behaviours, a feature not present in NGC 3115, NGC 7457, or even NGC 1023 from Cortesi et al. (2016). For all GC systems, there is no clear correlation between the component of the galaxy they are likely to belong to and their colour. We find also a population of GCs in NGC 3115 which are not likely to belong to any of the modelled components, within a confidence interval of 2.3σ. Those GCs could be related to a recent accretion event or to components not explicitly included in our model, such as the halo. This is to be further investigated.

In summary, this work shows that the structure and kinematics of lenticular galaxies in low-density environments is very diverse and more complex than expected by most formation scenarios proposed in the literature.

REFERENCES

Abadi M. G., Moore B., Bower R. G., 1999, MNRAS, 308, 947
Alabi A. B. et al., 2017, MNRAS, 468, 3949
Aragón-Salamanca A., 2008, in Bureau M., Athanassoula E., Barbuy B., eds, IAU Symposium Vol. 245, Formation and Evolution of Galaxy Bulges. pp 285
Aragón-Salamanca A., Bedregal A. G., Merrifield M. R., 2006, A&A, 458, 101
Arnold J. A. et al., 2014, ApJ, 791, 80
Ashman K. M., Bird C. M., Zepf S. E., 1994, AJ, 108, 2348
Bekki K., Couch W. J., Shioya Y., 2002, ApJ, 577, 651

Bekki K., Beasley M. A., Brodie J. P., Forbes D. A., 2005, MNRAS, 363, 1211

Borlaff A. et al., 2014, A&A, 570, A103

Boselli A., Gavazzi G., 2006, PASP, 118, 517

Bournaud F., Jog C. J., Combes F., 2005, A&A, 437, 69

Brodie J. P., Usher C., Conroy C., Strader J., Arnold J. A., Forbes D. A., Romanowsky A. J., 2012, ApJ, 759, L33

Brodie J. P. et al., 2014, ApJ, 796, 52

Buta R., Laurikainen E., Salo H., Knapen J. H., 2010, ApJ, 721, 259

Byrd G., Valtonen M., 1990, ApJ, 350, 89

Cantiello M., Blakeslee J. P., Raimondo G., Chies-Santos A. L., Jennings Z. G., Norris M. A., Kuntschner H., 2014, A&A, 564, L3

Ceverino D., Dekel A., Tweed D., Primack J., 2015, MNRAS, 447, 3291

Chomiuk L., Strader J., Brodie J. P., 2008, AJ, 136, 234

Coccato L. et al., 2009, MNRAS, 394, 1249

Cortesi A. et al., 2011, MNRAS, 414, 642

Cortesi A. et al., 2013, MNRAS, 432, 1010

Cortesi A. et al., 2016, MNRAS, 456, 2611

Côté P., McLaughlin D. E., Cohen J. G., Blakeslee J. P., 2003, ApJ, 591, 850

de Vaucouleurs G., de Vaucouleurs A., Corwin H. G. Jr. Buta R. J., Paturel G., Fouqué P., 1991, Third Reference Catalogue of Bright Galaxies. Volume I: Explanations and references. Volume II: Data for galaxies between 0^h and 12^h. Volume III: Data for galaxies between 12^h and 24^h, Springer, New York, NY, USA

Douglas N. G. et al., 2002, PASP, 114, 1234

Doyle M. T. et al., 2005, MNRAS, 361, 34

Dressler A., 1980, ApJ, 236, 351

Dressler A., Sandage A., 1983, ApJ, 265, 664

Dressler A. et al., 1997, ApJ, 490, 577

Dressler A. et al., 2011, PASP, 123, 288

Elmegreen B. G., Elmegreen D. M., 2005, ApJ, 627, 632

Emsellem E. et al., 2011, MNRAS, 414, 888

Faber S. M. et al., 2003, in Iye M., Moorwood A. F. M., eds, Proc. SPIE Vol. 4841, Instrument Design and Performance for Optical/Infrared Ground-based Telescopes. p. 1657

Fisher D. B. et al., 2017, ApJ, 839, L5

Forbes D. A., Brodie J. P., Grillmair C. J., 1997, AJ, 113, 1652

Forbes D. A. et al., 2012, MNRAS, 426, 975

Forbes D. A. et al., 2017, AJ, 153, 114

Fried J. W., Illingworth G. D., 1994, AJ, 107, 992

Garcia A. M., 1993, A&AS, 100, 47

Garland C. A., Pisano D. J., Mac Low M.-M., Kreckel K., Rabidoux K., Guzmán R., 2015, ApJ, 807, 134

Genzel R. et al., 2011, ApJ, 733, 101

Goto T., Yamauchi C., Fujita Y., Okamura S., Sekiguchi M., Smail I., Bernardi M., Gomez P. L., 2003, MNRAS, 346, 601

Guérou A., Emsellem E., Krajnović D., McDermid R. M., Contini T., Weilbacher P. M., 2016, A&A, 591, A143

Gunn J. E., Gott J. R., III, 1972, ApJ, 176, 1

Hanes D. A., Côté P., Bridges T. J., McLaughlin D. E., Geisler D., Harris G. L. H., Hesser J. E., Lee M. G., 2001, ApJ, 559, 812

Hargis J. R., Rhode K. L., Strader J., Brodie J. P., 2011, ApJ, 738, 113

Hui X., Ford H. C., Freeman K. C., Dopita M. A., 1995, ApJ, 449, 592

Hwang H. S. et al., 2008, ApJ, 674, 869

Inoue S., 2013, A&A, 550, A11

Kim D.-W., 1989, ApJ, 346, 653

Larson R. B., Tinsley B. M., Caldwell C. N., 1980, ApJ, 237, 692

McDermid R. M. et al., 2015, MNRAS, 448, 3484

Moody C. E., Romanowsky A. J., Cox T. J., Novak G. S., Primack J. R., 2014, MNRAS, 444, 1475

Norris M. A., Sharples R. M., Kuntschner H., 2006, MNRAS, 367, 815

Norris M. A. et al., 2014, MNRAS, 443, 1151

Oke J. B. et al., 1995, PASP, 107, 375

Oser L., Ostriker J. P., Naab T., Johansson P. H., Burkert A., 2010, ApJ, 725, 2312

Park H. S., Lee M. G., Hwang H. S., Kim S. C., Arimoto N., Yamada Y., Tamura N., Onodera M., 2012, ApJ, 759, 116

Peacock M. B., Zepf S. E., Kundu A., Maccarone T. J., Lehmer B. D., Gonzalez A. H., Maraston C., 2017, MNRAS, 466, 4021

Peng C. Y., Ho L. C., Impey C. D., Rix H.-W., 2002, AJ, 124, 266

Postman M. et al., 2005, ApJ, 623, 721

Pota V. et al., 2013, MNRAS, 428, 389

Querejeta M. et al., 2017, in Gil de Paz A., Knapen J. H., Lee J. C., eds, IAU Symposium Vol. 321, Formation and Evolution of Galaxy Outskirts. p. 114

Quilis V., Moore B., Bower R., 2000, Science, 288, 1617

Rhee J., Smith R., Choi H., Yi S. K., Jaffé Y., Candlish G., Sánchez-Jánssen R., 2017, ApJ, 843, 128

Rocha M., Peter A. H. G., Bullock J., 2012, MNRAS, 425, 231

Romanowsky A. J., Fall S. M., 2012, ApJS, 203, 17

Saha A., Armandroff T., Sawyer D. G., Corson C., 2000, in Iye M., Moorwood A. F., eds, Proc. SPIE Vol. 4008, Optical and IR Telescope Instrumentation and Detectors. p. 447

Sandage A., Bedke J., 1994, The Carnegie Atlas of Galaxies. Volumes I, II.

Savorgnan G. A. D., Graham A. W., 2016, ApJS, 222, 10

Shapiro K. L., Genzel R., Förster Schreiber N. M., 2010, MNRAS, 403, L36

Sil'chenko O. K., Afanasiev V. L., Chavushyan V. H., Valdes J. R., 2002, ApJ, 577, 668

Skrutskie M. F. et al., 2006, AJ, 131, 1163

Tully R. B. et al., 2013, AJ, 146, 86

van den Bergh S., 2009, ApJ, 702, 1502

van den Bergh S., Abraham R. G., Ellis R. S., Tanvir N. R., Santiago B. X., Glazebrook K. G., 1996, AJ, 112, 359

Whitmore B. C., Gilmore D. M., Jones C., 1993, ApJ, 407, 489

This paper has been typeset from a TEX/LATEX file prepared by the author.